IEEE Access
Multidisciplinary : Rapid Review : Open Access Journal

Received December 9, 2020, accepted December 15, 2020, date of publication December 24, 2020, date of current version January 5, 2021.

Digital Object Identifier 10.1109/ACCESS.2020.3047121

All-Optical Temporal Differentiator Based on the Axis-Aligned SFS Fiber Structure Filter

TINGYA YIN, (Student Member, IEEE), SEN ZHANG, TIANHAO ZHAO, AND WENHUA REN
Key Laboratory of All Optical Network and Advanced Telecommunication Network of EMC, Institute of Lightwave Technology, Beijing Jiaotong University, Beijing 100044, China

Corresponding author: Wenhua Ren (whren@bjtu.edu.cn)

This work was supported in part by the Fundamental Research Funds for the Central Universities, China, under Grant 2019JBM012, and in part by the National Natural Science Foundation of China under Grant 62075008 and Grant 61827818.

ABSTRACT In this paper, the axis-aligned single mode- four mode- single mode (SFS) fiber structure filter is proposed to be an all-optical temporal differentiator. It's shown that differentiators with different orders can be achieved by adjusting the parameters of the axis-aligned SFS fiber structure filter. All-optical temporal differentiators with orders of 0.375, 0.77 and 1 are obtained by using the axis-aligned SFS fiber structure filter, of which processing errors are 8.08%, 2.81%, 0.74%, respectively. The proposed design provides an easy and competitive way for the realization of the all-optical temporal differentiator.

INDEX TERMS Optical signal processing, optical pulse shaping, optical fiber devices.

I. INTRODUCTION

With the rapid development of data services, such as cloud computing and big data, the demand for processing massive amounts of information continues to increase. However, information processing still depends on microelectronics technology, which leads to many difficulties such as optical-electrical-optical (OEO) bottleneck and large power consumption. All-optical signal processing could overcome these difficulties, since it could provide larger bandwidth and higher computing speed. Therefore, all-optical signal processing has attracted considerable attentions in the past decades [1]–[4].

An effective implementation of all-optical signal processing is to imitate the development of electrical signal processing, building corresponding optical modules with the same functions, such as logical operations, differential operations and integral operations[5]. As an important device of the all-optical signal processing circuit, the all-optical temporal differentiator is used to obtain the differentiation of the input optical signal in the optical domain directly [6], which has extensive applications in the fields of ultra-short optical pulse shaping, ultra-high-speed coding, ultra-high-speed inductive control, and waveform detection [7]–[9].

The transfer function of an ideal N-th differentiator is $H_N(\omega) = [i(\omega\text{-}\omega_0)]^N$, which has a magnitude response of $|\omega\text{-}\omega_0|^N$ and a phase shift of $N\pi$ at ω_0, where ω refers to the optical frequency, ω_0 refers to the carrier frequency, and N can be an integer or a fraction. For example, for the first order all-optical temporal differentiator, the transfer function depends linearly on the baseband frequency, and there is a phase shift of π at the carrier frequency ω_0 [1].

In order to realize an N-th all-optical temporal differentiator, one should find an optical device whose transfer function is close to the ideal N-th differentiator. In fact, the differentiator can be considered as a band-stop filter near the carrier frequency. Different optical filters have been proposed to be an optical temporal differentiator, including integer-order and fractional-order differentiators, such as the Mach-Zehnder interferometer [10]–[13], Bragg grating [14]–[17], long-period grating [18], [19], microring resonator [20]–[22] and directional coupler [23]–[25].

The single mode- few mode- single mode (SFS) fiber structure filter is also a typical optical filter and has been widely used in fiber sensing in recent years [26]–[31]. In this paper, we will show that the SFS fiber structure filter can also work as an all-optical temporal differentiator.

Among all the SFS fiber structures, the axis-aligned SFS fiber structure, in which only the circular-symmetric modes $LP_{0\,n}$ can be excited, has the advantages of easy to manufacture and high stable [32]. The simplest axis-aligned SFS fiber structure filter is single mode- four mode- single mode (SFS) fiber structure. As an example, the SFS fiber structure filter is designed to be the all-optical temporal differentiator in this paper. It will be shown that differentiators with different orders can be achieved by adjusting the parameters of the SFS

The associate editor coordinating the review of this manuscript and approving it for publication was Wen Chen.

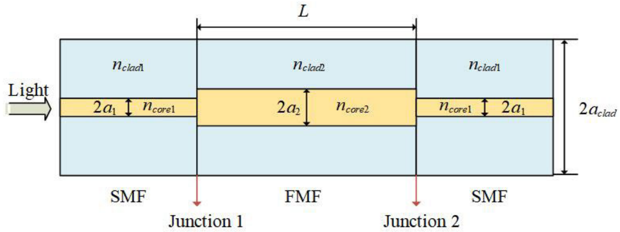

FIGURE 1. Schematic diagram of the axis-aligned SFS fiber structure.

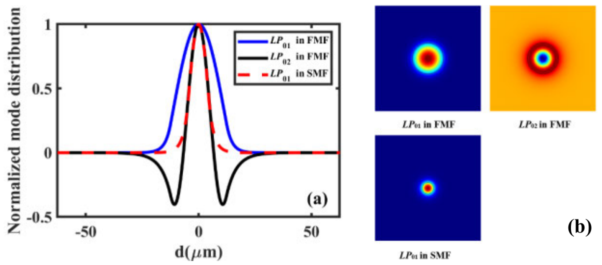

FIGURE 2. (a) The cross-section view and (b) top view of the mode distribution in the SMF and FMF. Parameters of the SMF are $a_1 = 4.5$ μm, $n_{core1} = 1.444$, $n_{clad1} = 1.4381$. Parameters of the FMF are $a_2 = 12.5$ μm, $n_{core2} = 1.444$, $n_{clad2} = 1.4405$.

fiber structure, which provides an easy and competitive way for the realization of the all-optical temporal differentiator. It should be noted that the SFS refers to single mode- four mode- single mode in the following.

The paper is organized as follows. In section II, the principle of the all-optical temporal differentiator based on the axis-aligned SFS fiber structure filter is presented. In section III, the all-optical temporal differentiator based on SFS fiber structure filter with different orders is designed and discussed. Finally, a conclusion is drawn in section IV.

II. PRINCIPLE

An axis-aligned SFS fiber structure consists of three segments: the single mode fiber (SMF), four mode fiber (FMF) and single mode fiber (SMF), as shown in Fig.1, where n_{core1} and n_{clad1} represent the refractive index of core and cladding of the SMF, n_{core2} and n_{clad2} represent the refractive index of core and cladding of the FMF.

At the first junction, the power carried by the fundamental mode (LP_{01}) in the first section of SMF is coupled into the FMF, where LP_{01} and LP_{02} modes are excited and propagate separately. At the second junction, the LP_{01} and LP_{02} modes will be coupled to the LP_{01} mode of the second section of SMF. Due to the different propagation constants of LP_{01} and LP_{02} modes in the FMF, an interference between them will occur at the second junction.

The power coupling coefficient in each junction between LP_{0n} ($n = 1, 2$) modes in the FMF and LP_{01} mode in the SMF can be expressed as [33]–[35]

$$\eta_{i,0n} = \frac{\left(\int_0^{2\pi}\int_0^{\infty}\psi_{s,i}(r,\varphi)\psi_{0n}^{*}(r,\varphi)\,rdrd\varphi\right)^2}{\int_0^{2\pi}\int_0^{\infty}\left|\psi_{s,i}(r,\varphi)\right|^2 rdrd\varphi\int_0^{2\pi}\int_0^{\infty}\left|\psi_{0n}(r,\varphi)\right|^2 rdrd\varphi} \tag{1}$$

where $\psi_{s,i}$ ($i = 1, 2$) and $\psi_{0\,n}$ represent the mode distribution of the LP_{01} mode in the SMF and the $LP_{0\,n}$ mode in the FMF, respectively. The subscript i means the i-th junction (for $\eta_{i,0n}$) and the i-th segment of SMF (for $\psi_{s,i}$). The filed distribution of mode $LP_{0\,n}$ in a circular-symmetric step-index fiber can be described with Bessel functions as

$$\psi_{0n}(r,\varphi) = \begin{cases} AJ_0(\frac{U_{0n}}{a}r), & r < a \\ A\dfrac{J_0(U_{0n})}{K_0(W_{0n})}K_0(\frac{W_{0n}}{a}r), & r \geq a \end{cases} \tag{2}$$

where a is the core radius of the fiber, $U_{0\,n}$ and $W_{0\,n}$ refer to the normalized transverse propagation constant, A is a constant related to optical power P carried by the corresponding mode. Fig.2 shows the cross-section view (a) and top view (b) of the mode distribution in the SMF and FMF, which are obtained by using the Comsol Multiphysics software. The corresponding power coupling coefficients are $\eta_{01} = 0.60$ and $\eta_{02} = 0.31$, which are calculated by using the Eq. (2).

At the end of the FMF segment with a length of L, the field distribution can be expressed as[32]

$$\mathrm{E}_{FMF} = \sum_{\mathrm{n}=1}^{2}\sqrt{\eta_{i,0n}}\psi_{0n}(r,\varphi)\exp(j\beta_{0n}L) \tag{3}$$

where $\beta_{0\,n}$ is the propagation constant of the $LP_{0\,n}$ mode. Therefore, the transfer function of the SFS fiber structure filter can be written as

$$H = \eta_{01} + \eta_{02}\exp\left[j\left(\beta_{02} - \beta_{01}\right)L\right] \tag{4}$$

In order to investigate the propagation characteristic of the axis-aligned SFS fiber structure, simulations are carried out with three different groups of parameters: $\eta_{01} = 0.61$, $\eta_{02} = 0.28$; $\eta_{01} = 0.47$, $\eta_{02} = 0.39$; $\eta_{01} = 0.50$, $\eta_{02} = 0.50$. The simulation results are shown in Fig. 3. As shown in Fig. 3(a1), (b1) and (c1), the propagation characteristic of the axis-aligned SFS fiber structure is a band-stop filter. As also can be seen from Fig. 3(a2), (b2) and (c2), there is an abrupt phase change near the center frequency. These response curves correspond to the all-optical temporal differentiator. The propagation characteristic of corresponding ideal differentiators that have the most similar amplitude and phase responses are also plotted in Fig. 3 with red dashed lines. The simulation results of the response in Fig. 3 are obtained by using the Matlab software.

Seen from Fig. 3, an ideal optical differentiator requires complete power extinction at the signal central frequency. While for the SFS fiber structure filter, the complete power extinction at the signal central frequency does not always occur. In fact, the complete power extinction at the signal central is a special case and need to be designed properly, when the SFS fiber structure filter works as a first order optical differentiator. This is one of the main causes of the processing error of the SFS fiber structure based optical differentiator.

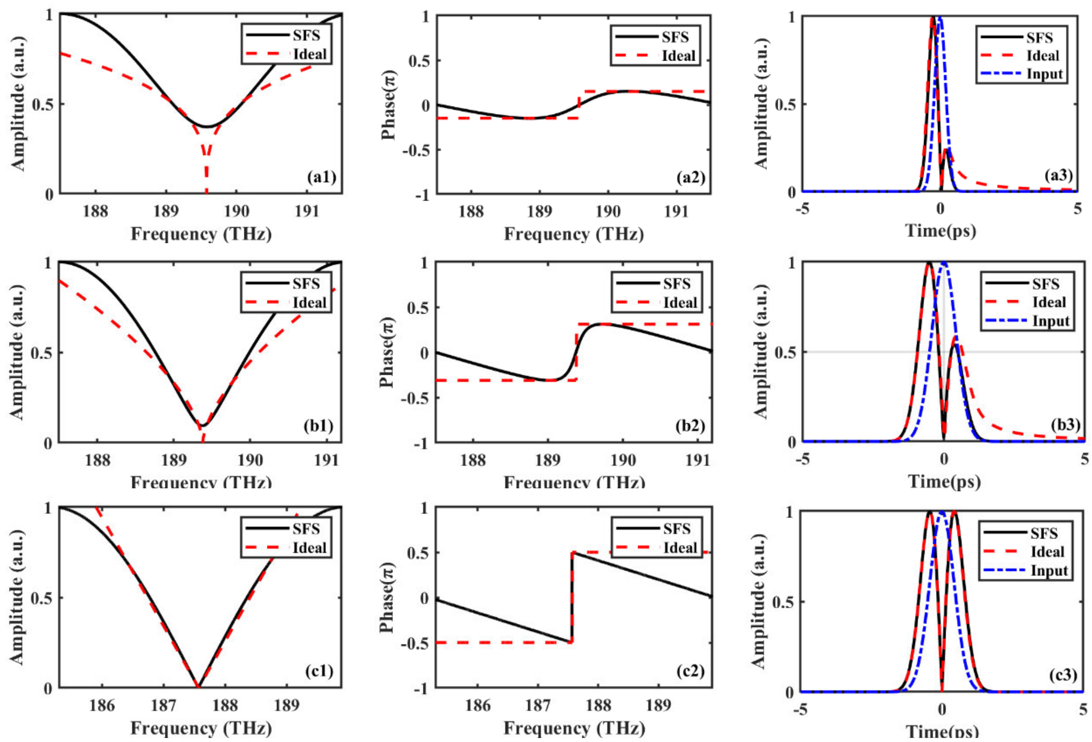

FIGURE 3. (a1), (b1) and (c1) represent the amplitude responses of the axis-aligned SFS fiber structure (solid lines) with different parameters: $\eta_{01} = 0.61$, $\eta_{02} = 0.28$; $\eta_{01} = 0.47$, $\eta_{02} = 0.39$; $\eta_{01} = 0.50$, $\eta_{02} = 0.50$. (a2), (b2) and (c2) represent the corresponding phase responses (solid lines). (a3), (b3) and (c3) represent the differentiation results with a Gaussian pulse input. The red dashed lines are the propagation characteristics of corresponding ideal differentiators that have the most similar amplitude and phase responses. The blue dashed lines are the incident pulses with FWHM of 0.47ps, 0.70ps, 1ps, respectively.

The order N of the all-optical temporal differentiator based on the axis-aligned SFS fiber structure can be obtained as[10]

$$N = \frac{\max[\varphi(H)] - \min[\varphi(H)]}{\pi} = \frac{2}{\pi}\arctan\frac{1}{\sqrt{\left(\frac{\eta_{01}}{\eta_{02}}\right)^2 - 1}} \tag{5}$$

where $\varphi(H)$ is the phase of H, and $\eta_{01} \geq \eta_{02}$. Especially when $\eta_{01} = \eta_{02}$, $N = 1$.

As indicated by Eq. (5), the order N of the all-optical temporal differentiator based on the axis-aligned SFS fiber structure filter is determined by the power coupling coefficients η_{01} and η_{02}. Fig. 4 shows the order of the all-optical temporal differentiator based on the SFS fiber structure filter with different η_{01} and η_{02}, where $\eta_{01} \geq \eta_{02}$. In general, a given axis-aligned SFS fiber structure filter is able to work as an all-optical temporal differentiator with a fixed order. In order to work as an all-optical temporal differentiator with some specific order, the parameters of the axis-aligned SFS fiber structure filter should be designed carefully, i.e. diameters and refractive indices of the single-mode-fiber and four-mode-fiber. The best way is to fabricate the fibers oneself, which is impractical for most labs. In practice, we could collect the parameters of commercial fibers from different companies and pick out the suitable ones. Also we can

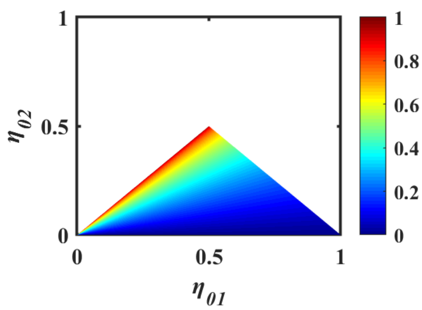

FIGURE 4. The order of the all-optical temporal differentiator based on the SFS fiber structure filter with different power coupling coefficients η_{01} and η_{02}.

process the commercial fibers by using special equipment, e.g. the LZM100 Laser Maser of Fujikura.

III. SIMULATIONS AND DISCUSSIONS

In order to investigate the performance of the all-optical temporal differentiator based on the axis-aligned SFS fiber structure filter, three groups of parameters are used to carry out simulations. The parameters of the SMF are the same among the three groups, which are $a_1 = 4.5\ \mu$m, $n_{core1} = 1.449$, $n_{clad1} = 1.444$. The parameters of the FMF are (1) $a_2 = 16\ \mu$m, $n_{core2} = 1.4456$, $n_{clad2} = 1.444$, $L = 0.08$ m, (2) $a_2 = 20\ \mu$m, $n_{core2} = 1.4455$, $n_{clad2} = 1.444$,

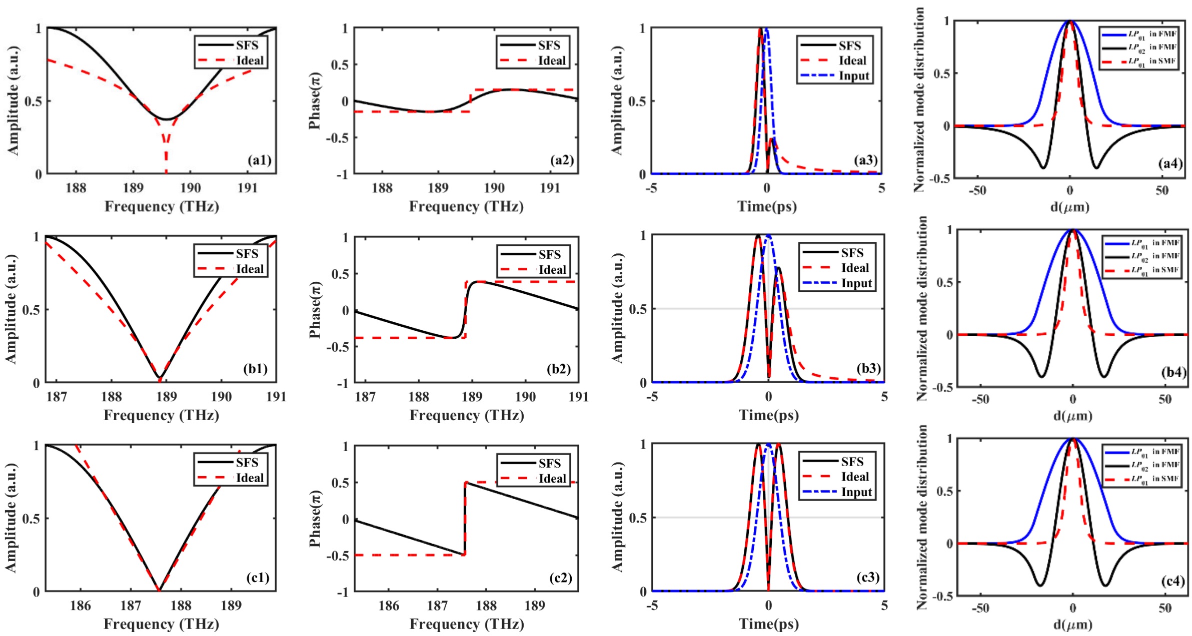

FIGURE 5. (a1), (b1) and (c1) represent the amplitude responses of the axis-aligned SFS fiber structure (solid lines) with different parameters of the FMF: (1) $a_2 = 16\ \mu$m, $n_{core2} = 1.4456$, $n_{clad2} = 1.444$, L = 0.08 m, (2) $a_2 = 20\ \mu$m, $n_{core2} = 1.4455$, $n_{clad2} = 1.444$, L = 0.08 m. (3) $a_2 = 21\ \mu$m, $n_{core2} = 1.4454$, $n_{clad2} = 1.444$, L = 0.08 m. (a2), (b2) and (c2) represent the corresponding phase responses (solid lines). (a3), (b3) and (c3) represent the differentiation results with a Gaussian pulse input. The red dashed lines are the propagation characteristics of the ideal differentiators. The blue dashed lines are the incident pulses with FWHM of 0.66ps, 1ps, 1ps, respectively. (a4), (b4) and (c4) represent the cross-section view of the mode distribution in the FMF.

$L = 0.08$ m. (3) $a_2 = 21\ \mu$m, $n_{core2} = 1.4454$, $n_{clad2} = 1.444$, $L = 0.08$ m.

The amplitude and phase response of the axis-aligned SFS fiber structure filter with the above parameters are shown in Fig. 5 with solid lines. The differential order of the axis-aligned SFS fiber structure filter can be obtained by calculating the power coupling coefficients and using the Eq. (5), which are 0.375, 0.77, 1, respectively. Also the corresponding ideal differentiators are plotted in Fig. 5 with red dashed lines as a contrast. Seen from Fig. 5, the response of the axis-aligned SFS fiber structure filter accord well with that of the corresponding ideal differentiators.

Fig. 5 (a3), (b3) and (c3) show the differentiation results when a Gaussian pulse is launched to the above designed axis-aligned SFS fiber structure based all-optical temporal differentiators. The FWHM of the input Gaussian pulses are 0.66ps, 1ps, 1ps, respectively. We can clearly see that the obtained output results accord well with the ideal output results.

Also we can see that the output of the axis-aligned SFS fiber structure based all-optical temporal differentiator is two sub-pulses, both of which are narrower than the incident pulse. What's more, the FWHM of the sub-pulse with a smaller amplitude is a little wider than that of the sub-pulse with a bigger amplitude.

In order to analyze the differentiation results quantificationally, usually the processing error (D) is introduced, which is defined as [7], [36]

$$\mathrm{D} = \frac{\int \left| |f(t)|^2 - |g(t)|^2 \right| dt}{\int |g(t)|^2\, dt}, \tag{6}$$

where the $f(t)$ refers to the output of the proposed differentiator, $g(t)$ refers to the output of the ideal differentiator, and both signals have been normalized. The calculated processing errors of the three designed axis-aligned SFS fiber structure based differentiators with orders of 0.375, 0.77, 1 are 8.08%, 2.81%, 0.74%, respectively, which show excellent differential performance.

The principle of the axis-aligned SFS fiber structure based all-optical temporal differentiator can be understood as follows. The input pulse is divided into two pulses at the first junction, which are carried by the LP_{01} and LP_{02} modes of the FMF independently. Due to the different propagation velocities, the pulse carried by the LP_{01} mode arrives at the second junction earlier than the pulse carried by the LP_{02} mode. If the length of the FMF is designed properly, there will be two separate pulses in the second segment of the SMF. If $\eta_{01} > \eta_{02}$, the earlier pulse (carried by the LP_{01} mode) has a bigger amplitude than the later pulse (carried by the LP_{02} mode), which accords with the differentiator with an order $N < 1$. If $\eta_{01} = \eta_{02}$, the earlier pulse has the same amplitude as the later pulse, which accords with the differentiator with an order $N = 1$.

Seen from Fig.3 and Fig. 5, the center wavelength of the differentiator can be different when the design parameters are changed. The center wavelength is quite an important parameter for the all optical differentiator. When the center wavelength of the differentiator deviates from that of the incident signal, the processing error will increase with the deviation. The allowable deviation of the center wavelength is determined by the allowable processing error. So the center wavelength of the differentiator should be controlled precisely.

Normally stress and temperature are the main influencing factors for the shifting of the center wavelength. So the stress or temperature adjusting devices can be utilized to adjust the center wavelength of the differentiator. If we want the center wavelength to be fixed, the SFS fiber structure based differentiator can be packed using some special material with negative temperature coefficient. Also some precise feedback systems can be utilized to control the center wavelength.

It should be noted that we didn't consider the length of the SMF1 and SMF2 here, because the chromatic dispersion in the SMF is quite smaller than the mode dispersion in the FMF. However, the length of the SMFs should be considered in the actual experiment, especially when the incident optical pulse is an ultrashort pulse, i.e. picosecond pulse or sub-picosecond pulse.

In order to fabricate an SFS fiber structure, we need to splice two sections of SMF to the two ends of a section of FMF. Usually a broadband light source is launched into one end of the SFS structure and an optical spectrum analyzer (OSA) is connected to the other end of the SFS structure to detect the output spectrum. It's better to utilize two fiber fusion splicers during the fabrication of the SFS fiber structure. So the two fiber fusion splicing points can be adjusted and fusion spliced at the same time to make sure the transfer function is what we need.

What's more, from the above analysis, the order of the axis-aligned SFS fiber structure based all-optical temporal differentiator is mainly determined by the transverse parameters of the SMS and FMF, including the core indices, cladding indices, core radii, cladding radii, etc. The processing bandwidth is mainly determined by the length of the FMF. So the parameters of the SMF and FMF should be chosen carefully.

IV. CONCLUSION

In conclusion, the axis-aligned SFS fiber structure filter is proposed to be an all-optical temporal differentiator in this paper. The order of the all-optical temporal differentiator can be 0~1 by adjusting the power coupling coefficients at the junctions in the axis-aligned SFS fiber structure, which are determined by the parameters of the SMF and FMF. Three all-optical temporal differentiators with orders of 0.375, 0.77 and 1 are designed based on the axis-aligned SFS fiber structure filter. The processing errors are 8.08%, 2.81%, 0.74%, respectively, which show excellent differential performance. The axis-aligned SFS fiber structure filter has the advantages of easy to manufacture and high stable, which provide a competitive way for the realization of the all-optical temporal differentiator.

REFERENCES

[1] J. Azaa, "Ultrafast analog all-optical signal processors based on fiber-grating devices," *IEEE Photon. J.*, vol. 2, no. 3, pp. 359–386, Jun. 2010.

[2] J. Dong, M. Liu, S. Gao, X. Zhang, X. Cai, and X. Wang, "Widely tunable fractional-order photonic differentiator using a Mach-Zenhder interferometer coupled microring resonator," *Opt. Exp.*, vol. 25, no. 26, pp. 33305–33314, Dec. 2017.

[3] X. Liu and X. Shu, "Design of an all-optical fractional-order differentiator with terahertz bandwidth based on a fiber Bragg grating in transmission," *Appl. Opt.*, vol. 56, no. 24, pp. 6714–6719, Aug. 2017.

[4] T. Wu, C. Zhang, H. Zhou, H. Huang, and K. Qiu, "Photonic microwave waveforms generation based on frequency and time-domain synthesis," *IEEE Access*, vol. 6, pp. 34372–34379, 2018.

[5] C.-W. Hsue, L.-C. Tsai, and K.-L. Chen, "Implementation of first-order and second-order microwave differentiators," *IEEE Trans. Microw. Theory Techn.*, vol. 52, no. 5, pp. 1443–1448, May 2004.

[6] T.-J. Ahn and J. Azaña, "Wavelength-selective directional couplers as ultrafast optical differentiators," *Opt. Exp.*, vol. 19, no. 8, pp. 7625–7632, Jul. 2011.

[7] M. Kulishov and J. Azaña, "Long-period fiber gratings as ultrafast optical differentiators," *Opt. Lett.*, vol. 30, no. 20, pp. 2700–2702, Oct. 2005.

[8] J. Yao, F. Zeng, and Q. Wang, "Photonic generation of ultrawideband signals," *J. Lightw. Technol.*, vol. 25, no. 11, pp. 3219–3235, Nov. 2007.

[9] M. A. Preciado and M. A. Muriel, "Design of an ultrafast all-optical differentiator based on a fiber Bragg grating in transmission," *Opt. Lett.*, vol. 33, no. 21, pp. 2458–2460, Dec. 2008.

[10] C. Cuadrado-Laborde, "All-optical ultrafast fractional differentiator," *Opt. Quantum Electron.*, vol. 40, no. 13, pp. 983–990, Oct. 2008.

[11] Y. Yu, F. Jiang, H. Tang, L. Xu, X. Liu, J. Dong, and X. Zhang, "Reconfigurable photonic temporal differentiator based on a dual-drive Mach-Zehnder modulator," *Opt. Exp.*, vol. 24, no. 11, pp. 11739–11748, May 2016.

[12] A. Zheng, T. Yang, X. Xiao, Q. Yang, X. Zhang, and J. Dong, "Tunable fractional-order differentiator using an electrically tuned silicon-on-isolator Mach-Zehnder interferometer," *Opt. Exp.*, vol. 22, no. 15, pp. 18232–18237, Jul. 2014.

[13] J. Dong, A. Zheng, D. Gao, L. Lei, D. Huang, and X. Zhang, "Compact, flexible and versatile photonic differentiator using silicon Mach-Zehnder interferometers," *Opt. Exp.*, vol. 21, no. 6, pp. 7014–7024, Mar. 2013.

[14] X. Liu, X. Shu, and H. Cao, "Proposal of a phase-shift fiber Bragg grating as an optical differentiator and an optical integrator simultaneously," *IEEE Photon. J.*, vol. 10, no. 3, pp. 1–7, Jun. 2018.

[15] M. Li, L.-Y. Shao, J. Albert, and J. Yao, "Continuously tunable photonic fractional temporal differentiator based on a tilted fiber Bragg grating," *IEEE Photon. Technol. Lett.*, vol. 23, no. 4, pp. 251–253, Feb. 2011.

[16] H. Shahoei, J. Albert, and J. Yao, "Tunable fractional order temporal differentiator by optically pumping a tilted fiber Bragg grating," *IEEE Photon. Technol. Lett.*, vol. 24, no. 9, pp. 730–732, May 2012.

[17] M. Wang and J. Yao, "Tunable 360° photonic radio-frequency phase shifter based on polarization modulation and all-optical differentiation," *J. Lightw. Technol.*, vol. 31, no. 15, pp. 2584–2589, Aug. 2013.

[18] R. Ashrafi, M. H. Asghari, and J. Azana, "Ultrafast optical arbitrary-order differentiators based on apodized long-period gratings," *IEEE Photon. J.*, vol. 3, no. 3, pp. 353–364, Jun. 2011.

[19] C. Cuadrado-Laborde and M. V. Andrés, "Design of an ultra-broadband all-optical fractional differentiator with a long-period fiber grating," *Opt. Quantum Electron.*, vol. 42, nos. 9–10, pp. 571–576, Jun. 2011.

[20] F. Liu, T. Wang, L. Qiang, T. Ye, and Y. Su, "Compact optical temporal differentiator based on silicon microring resonator," *Opt. Exp.*, vol. 16, no. 20, pp. 15880–15886, 2008.

[21] A. Zheng, J. Dong, L. Zhou, X. Xiao, Q. Yang, and X. Zhang, "Fractional-order photonic differentiator using an on-chip microring resonator," *Opt. Lett.*, vol. 39, no. 21, pp. 6355–6358, Nov. 2014.

[22] W. Zhang, W. Liu, W. Li, H. Shahoei, and J. Yao, "Independently tunable multichannel fractional-order temporal differentiator based on a silicon-photonic symmetric Mach–Zehnder interferometer incorporating cascaded microring resonators," *J. Lightw. Technol.*, vol. 33, no. 2, pp. 361–367, Jan. 15, 2015.

[23] S. Sun, M. Li, J. Tang, and N. Zhu, "Femtosecond pulse shaping using wavelength-selective directional couplers: Proposal and simulation," *Opt. Exp.*, vol. 24, no. 8, pp. 7943–7950, Apr. 2016.

[24] T.-T. Yan, W.-H. Ren, and Y.-C. Jiang, "Asymmetric wavelength-selective directional couplers as fractional-order optical differentiators," *IEEE Access*, vol. 7, pp. 56533–56538, 2019.

[25] H.-S. Jeong, C.-Y. Kim, W. Shin, and T.-J. Ahn, "Dual-wavelength first-order optical differentiators based on bidirectional fiber couplers," *J. Opt.*, vol. 15, no. 5, May 2013, Art. no. 055405.

[26] W. Liu, X. Wu, G. Zhang, S. Li, C. Zuo, W. Zhang, and B. Yu, "Thin fiber-based Mach-Zehnder interferometric sensor for measurement of liquid level, refractive index, temperature, and axial strain," *Appl. Opt.*, vol. 59, no. 6, pp. 1786–1792, Feb. 2020.

[27] X. Yu, D. Bu, X. Chen, J. Zhang, and S. Liu, "Lateral stress sensor based on an in-fiber Mach–Zehnder interferometer and Fourier analysis," *IEEE Photon. J.*, vol. 8, no. 2, pp. 1–10, Apr. 2016.
[28] X. Gao, T. Ning, C. Zhang, J. Xu, J. Zheng, H. Lin, J. Li, L. Pei, and H. You, "A dual-parameter fiber sensor based on few-mode fiber and fiber Bragg grating for strain and temperature sensing," *Opt. Commun.*, vol. 454, Jan. 2020, Art. no. 124441.
[29] T. Huang, X. Shao, Z. Wu, Y. Sun, J. Zhang, H. Q. Lam, J. Hu, and P. P. Shum, "A sensitivity enhanced temperature sensor based on highly germania-doped few-mode fiber," *Opt. Commun.*, vol. 324, pp. 53–57, Aug. 2014.
[30] J. Liu, M. Wang, X. Liang, Y. Dong, H. Xiao, and S. Jian, "Erbium-doped fiber ring laser based on few-mode-singlemode-few-mode fiber structure for refractive index measurement," *Opt. Laser Technol.*, vol. 93, pp. 74–78, Aug. 2017.
[31] J. Su, X. Dong, and C. Lu, "Property of bent few-mode fiber and its application in displacement sensor," *IEEE Photon. Technol. Lett.*, vol. 28, no. 13, pp. 1387–1390, Jul. 1, 2016.
[32] J. Zheng, L. Pei, T. Ning, J. Li, C. Zhang, S. Ma, and Z. Ruan, "Matching optimization for SFS-structured interferometers with step-index fibers," *Opt. Exp.*, vol. 26, no. 7, pp. 9182–9193, 2018.
[33] Q. Wang and G. Farrell, "All-fiber multimode-interference-based refractometer sensor: Proposal and design," *Opt. Lett.*, vol. 31, no. 3, pp. 317–319, 2006.
[34] Q. Wu, Y. Semenova, P. Wang, and G. Farrell, "High sensitivity SMS fiber structure based refractometer-analysis and experiment," *Opt. Exp.*, vol. 19, no. 9, pp. 7937–7944, 2011.
[35] H. Li, G. Ren, S. Atakaramians, B. T. Kuhlmey, and S. Jian, "Linearly polarized single TM mode terahertz waveguide," *Opt. Lett.*, vol. 41, no. 17, pp. 4004–4007, Sep. 2016.
[36] H. You, T. Ning, W. Jian, L. Pei, X. Wen, J. Li, and H. Chen, "Optical temporal differentiator using a twin-core fiber," *Opt. Eng.*, vol. 52, no. 1, Jan. 2013, Art. no. 015005.

TINGYA YIN (Student Member, IEEE) received the bachelor's degree from Beijing Jiaotong University, in 2019, where she is currently pursuing the master's degree. Her research interests include optical device and optical signal processing.

SEN ZHANG received the bachelor's degree from the North University of China, in 2018. She is currently pursuing the master's degree with Beijing Jiaotong University. Her research interests include optical device and optical signal processing.

TIANHAO ZHAO received the bachelor's degree from the Hefei University of Technology, in 2018. He is currently pursuing the master's degree with Beijing Jiaotong University. His research interests include optical device and optical signal processing.

WENHUA REN received the bachelor's and Ph.D. degrees from Beijing Jiaotong University, China, in 2005 and 2010, respectively. He is currently an Associate Professor with the Institute of Lightwave Technology, Beijing Jiaotong University. His research interests include special optical fiber and optical fiber lasers.